



## OSL and EPR dating of pottery from the archaeological sites in Amazon Valley, Brazil



Nilo F. Cano <sup>a,b,\*</sup>, Casimiro S. Munita <sup>a</sup>, Shigaeo Watanabe <sup>b</sup>, Renata F. Barbosa <sup>b</sup>, José F.D. Chubaci <sup>b</sup>, Sonia H. Tatumi <sup>c</sup>, Eduardo G. Neves <sup>d</sup>

<sup>a</sup> Instituto de Pesquisas Energéticas e Nucleares IPEN-CNEN/SP, Av. Prof. Lineu Prestes 2242, CEP 05508-000 São Paulo, SP, Brazil

<sup>b</sup> Instituto de Física, Universidade de São Paulo, Rua do Matão, Travessa R, 187, CEP 05508-900 São Paulo, SP, Brazil

<sup>c</sup> Universidade Federal de São Paulo, Campus Baixada Santista, Av. Saldanha da Gama 89, Ponta da Praia, CEP 11030-400 Santos, SP, Brazil

<sup>d</sup> Museu de Arqueologia e Etnologia, Universidade de São Paulo, Av. Prof. Almeida Prado 1466, CEP 05508-900 São Paulo, SP, Brazil

### ARTICLE INFO

#### Article history:

Available online 4 June 2013

### ABSTRACT

Pottery fragments from the Hatahara archaeological site, Amazon Valley, have been dated by thermoluminescence (TL), optically stimulated luminescence (OSL) and electron paramagnetic resonance (EPR) techniques. X-ray diffraction measurements and optical microscopic observation revealed crystalline quartz grains and amorphous grains in the ceramics. These grains are in the form of needles and are spicules. The calculated ages are consistent with the period of occupation of the Hatahara archaeological site estimated by stratigraphical analysis.

© 2013 Elsevier Ltd and INQUA. All rights reserved.

### 1. Introduction

Thermoluminescence (TL), optically stimulated luminescence (OSL) and electron paramagnetic resonance (EPR) are methods used for dating pottery. These techniques make use of feldspar, quartz and other crystals present in the ceramics for dating (Aitken, 1985; Bartoll and Ikeya, 1997). In general, quartz grains are usually used in dating experiments.

In these dating techniques, two basic quantities must be measured: accumulated dose,  $D_{ac}$ , and annual dose rate,  $D_{an}$ . From the moment the fragment of pottery is buried in the soil by some process, the pottery is subjected to natural radiation due to radioactive nuclides in the pottery and soil. This irradiation continues until the moment the pottery fragment is collected for dating experiments. The accumulated dose by the fragment during this period is  $D_{ac}$ . The annual dose rate due to radiation from radionuclides in the pottery and soil is denoted by  $D_{an}$ . The dose rate is due to both nuclides in the pottery and in the soil plus cosmic rays contribution. The pottery nuclides contribute much more than do the soil nuclides.

In principle, if the thermoluminescence induced per unit dose (Gy) ( $TL_u$ ) is measured from the total thermoluminescence of quartz grains from the pottery ( $TL_0$ ),  $TL_0/TL_u$  gives  $D_{ac}$ . However, in

practice, the so-called additive dose method (alternative to regeneration method) is used. In this method, quartz grains from the pottery are irradiated with laboratory dose in the range of a few Gy to 50 Gy. The measured thermoluminescence from these grains is plotted as a function of dose. The accumulated dose  $D_{ac}$  is derived by extrapolating the plotted line to the negative dose axis. The annual dose rate  $D_{an}$  is estimated by measuring the concentrations of  $^{238}\text{U}$ ,  $^{232}\text{Th}$  in ppm and  $^{40}\text{K}$  in weight % in the sample and using, for example, Table 4.5 given by Ikeya (1993). From the measured values of  $D_{ac}$  and  $D_{an}$ , the age is determined by the relation  $D_{ac}/D_{an}$ .

The peoples in the central Amazon region lived in groups along the margins of rivers. For their daily necessities, they made many ceramic artifacts (pottery). The raw materials for making the potteries came from neighboring areas with clay material. To improve the plasticity properties of the raw material, the indigenous people intentionally added Cauxi (freshwater sponge) and Cariapé, supposed to make better ceramics, and therefore an important chemical aspect of the tempering. Evidence of organic tempering has been found in several ceramic fragments from central Amazon (Costa et al., 2004a).

Costa et al. (2004b) recognized that the freshwater sponge Cauxi, found in the Amazon basin, contains amorphous needle-like silica spicules. Sponge spicules can also be found dispersed in the soil, which could suggest that they were part of the clay source used to produce ceramics.

The Hatahara archaeological site is in the district of Iranduba, 30 km southwest of Manaus, Brazil. It is located on the left margin of the Solimões River near to the confluence of the Negro River

\* Corresponding author. Institute of Physics, University of São Paulo, Nuclear Physics Department, Rua do Matao, Travessa R, 187, CEP 05508-900 São Paulo, SP, Brazil.

E-mail addresses: [nilocano@if.usp.br](mailto:nilocano@if.usp.br), [nfcano@gmail.com](mailto:nfcano@gmail.com) (N.F. Cano).

(Rebellato, 2007). Machado (2005) has described the history of four distinct phases of occupation: Paredão, Manacapuru, Guarita, and Açu tuba. These phases were established by archaeological criteria, namely the decoration, form of the vessel, and mostly by the kind of tempering used in the paste. The use of such tempering depends upon local availability of the temper and the user. The kind of tempering used can characterize not only the site, but also the nature of inhabitants.

The present work aims at elucidating the effect of the spicules in pottery dating as carried out using the techniques of TL, OSL, and EPR. This can be done by comparing the luminescence and EPR spectra of crystalline quartz mixed with spicules with those of spicules alone. It is intended to confirm the chronology of the occupation of this site, as obtained by stratigraphy on the one hand and with ages of ceramics obtained by OSL and EPR techniques on the other.

## 2. Experimental

### 2.1. Samples

The archaeological samples used in this study are fragments of pottery collected by archaeologists from the MAE-USP (Museu de Arqueologia e Etnologia – Universidade de São Paulo) at the Hatahara archaeological site. Seven ceramics have been selected, each one representing seven different phases of occupation, following Nunes (2009). They were named CSNH-50, CSNH-67, CSNH-68, CSNH-69, CSNH-73, CSNH-78, and CSNH-93.

In order to observe the effects of the spicules on TL, OSL and EPR spectra, sponges with spicules were collected from the margin of the Solimões River. These sponges were prepared and analyzed in the same way as the potteries.

### 2.2. Chemical treatment

Approximately of 15 g of mass of each fragment of pottery was subjected to the following processes: (1) the surface was rubbed with sandpaper to remove a few mm of the surface layer to eliminate unknown effects that can interfere with the main measurements; (2) fragments were crushed and sieved to retain grain size between 0.080 and 0.180 mm; and (3) fragments were submitted to chemical treatment in solutions of  $H_2O_2$ , HCl, and HF. Grains with diameter smaller than 0.080 mm were used to find uranium, thorium and potassium content for internal annual dose rate measurements. They also were used for X-ray diffraction measurement. The chemical treatment has two purposes. One is to eliminate, although partially, organic and inorganic particles. The second purpose is to partially corrode the surface of quartz grains, such that the effect of  $\alpha$ -particles can be neglected. Watanabe et al. (2008) have shown that the optimum reaction time when using a solution of 40% HF and 37% HCl is 40 min, and this procedure was followed here.

Several papers have discussed chemical methods used to reduce the intensity of the EPR signal due to  $Fe^{3+}$  (Bensimon et al., 1998; Ferretti et al., 2002; Duttine et al., 2003). This  $Fe^{3+}$  signal is usually large and hides the E'-center signal used in EPR dating. In the present work, the method proposed by Watanabe et al. (2008) was used. With an additional chemical treatment with 40%  $HNO_3$  solution for 40 min followed by washing several times in Milli-Q water, it is possible to remove iron agglomerates by dilution.

### 2.3. Measuring apparatus

Pictures of ground samples were obtained using a digital camera attached to a Bioval, model L-1000T optical microscope. The XRD analysis was carried out utilizing a Rigaku diffractometer with  $Cu-K\alpha$  radiation and using a 10–90° scan range.

The TL measurements were carried out in a nitrogen atmosphere with a model 1100 Daybreak TL reader equipped with a photomultiplier (PMT) EMI 9235QA for light detection along with Corning 7-59 and Schott BG-39 filters used in front of the PMT. The heating rate used in the TL measurements was 4 C°/s. Each point in the glow curve represents an average of five readings.

The OSL measurements of the quartz samples were carried out using a Risø TL/OSL reader equipped with a  $^{90}Sr/^{90}Y$  beta particle source (Botter-Jensen et al., 2000). The reader uses a 9635QA photomultiplier tube. The stimulation wavelength is 470 nm. The detection optics consisted of a 7.5 mm Hoya U-340 filter.

A Bruker EMX EPR spectrometer operating at X-band frequency with 100 kHz modulation frequency was utilized for the EPR measurements. 100 mg of powdered sample was used for each measurement. Diphenyl picryl hydrazyl (DPPH) was used for calibration of the g values of the defect centers.

### 2.4. Gamma ray irradiation

The irradiations were carried out at the Center of Technology of Radiations of the Institute of Nuclear and Energy Research (CTR-IPEN), using a  $^{60}Co$   $\gamma$ -source with a dose rate of 19.7 Gy/h at room temperature and under conditions of electronic equilibrium.

## 3. Results and discussions

### 3.1. Mineralogical analysis

The OM photograph and the XRD pattern of the samples are shown in Figs. 1 and 2 respectively. Fig. 1(a) shows the OM picture

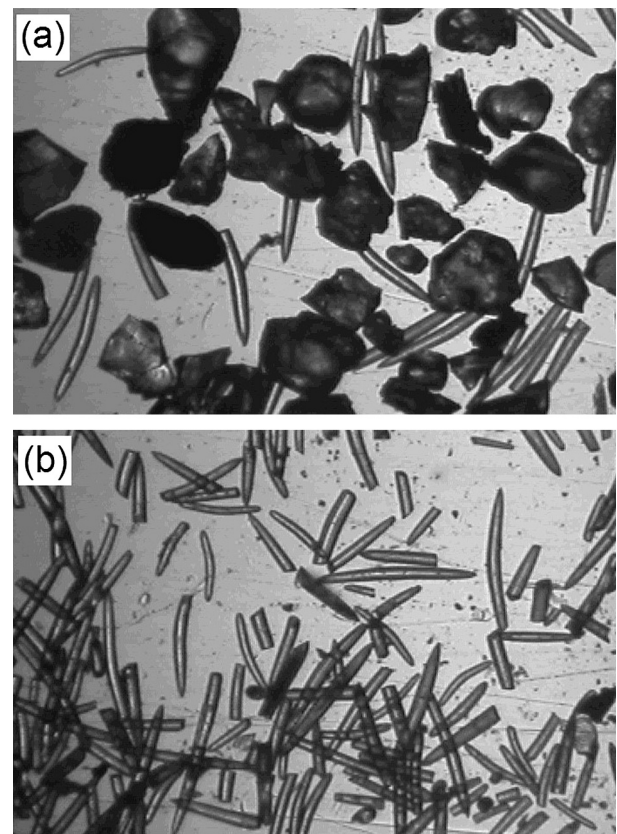
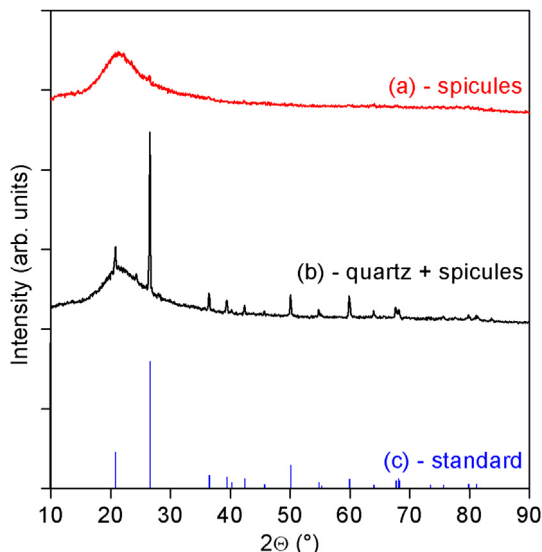


Fig. 1. (a) Optical microscopy image of quartz crystal mixed with spicules from pottery. (b) Optical microscopy image of spicules from freshwater sponge.



**Fig. 2.** Comparison of the powder X-ray diffraction of samples after chemical treatments: Quartz standard, quartz and spicules from pottery, spicules from freshwater sponges.

of a sample containing a mixture of quartz grains and spicules. **Fig. 1(b)** shows the OM photograph of a sample with spicules only. The X-ray diffraction pattern of spicules is given in **Fig. 2(a)**. **Fig. 2(b)** shows the X-ray diffraction pattern of a sample containing both quartz and spicules. The diffraction pattern of pure  $\alpha$ -quartz is shown in **Fig. 2(c)** for comparison.

### 3.2. TL measurements

The additive dose method was used to evaluate accumulated dose,  $D_{ac}$ . One aliquot of 3 mg sample was used in these experiments. **Fig. 3** shows the glow curves of sample CSNH-68 irradiated with additional  $\gamma$  doses varying from 2 to 15 Gy. The sample exhibits two TL peaks, one around 160 °C and another broad peak centered at 400 °C. As seen in the inset of **Fig. 3**, spicules produce a large peak at 400 °C and overlap the important 325 °C peak

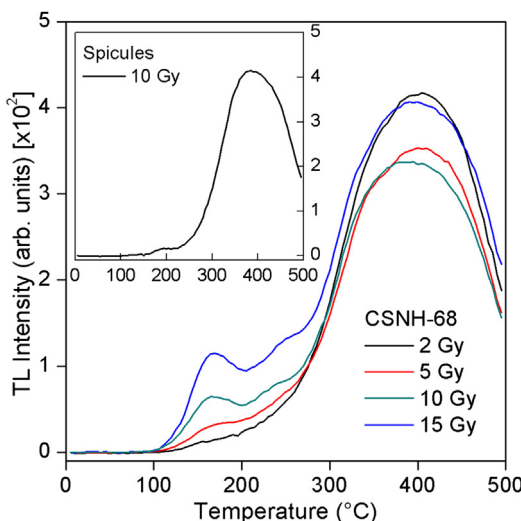


**Fig. 3.** TL glow curves of the natural and irradiated sample CSNH-68. In the inset of the figure, the TL glow curve of the spicules extracted from freshwater sponge irradiated to 10 Gy is shown.

observed in quartz. It is possible to obtain the 325 °C TL peak by subtracting the spicules glow curve from the corresponding glow curve in **Fig. 3**. Such a procedure was not carried out in the present study, as it is too time consuming.

### 3.3. OSL measurements

The accumulated dose was determined using a single aliquot regenerative-dose (SAR) procedure, the SAR-OSL protocol (Murray and Wintle, 2000, 2003). In this protocol, the first cycle is intended to measure the OSL signal of the natural sample, eliminating the energy accumulated since the last time the sample was exposed to light. A second cycle was performed to regenerate the OSL signal of the natural sample. In this cycle, different doses of radiation are given using a  $^{90}\text{Sr}/^{90}\text{Y}$   $\beta$  source, and the OSL signal (Li) is measured. A pre-heat of 220 °C was used to eliminate the 110 °C peak contribution. Sensitivity changes that occur during the regeneration process of the OSL signal in laboratory are checked by the OSL response to a test dose (Ti), which is always constant. The accumulated dose is calculated by interpolation of the curve Li/Ti in function dose. **Fig. 4** shows a typical SAR laboratory growth curve for one of the aliquots of the sample CSNH-86 and an OSL decay curve (**Fig. 4**, inset) for the sample CSNH-68 and spicules. The growth curve is fitted acceptably well to a linear equation. **Fig. 4** is a representative example of the luminescence characteristics exhibited by the samples, and illustrates their generally good behavior in the SAR protocol. Recycling ratios are indistinguishable from unity and the growth curves pass very close to the origin. Furthermore, this figure shows a comparison of the OSL signal of quartz grains and spicules of the pottery and OSL signal of pure spicules obtained from freshwater sponge. Both samples were irradiated with a gamma dose of 6 Gy. There is no interference of spicules on the OSL signal of quartz grains.

Histograms of accumulated dose distribution of sample CSNH-68 are shown in **Fig. 5**. All samples show reasonably tight and symmetrical distributions, after rejection of a few aliquots with high dose outliers which were considered as abnormal aliquots.

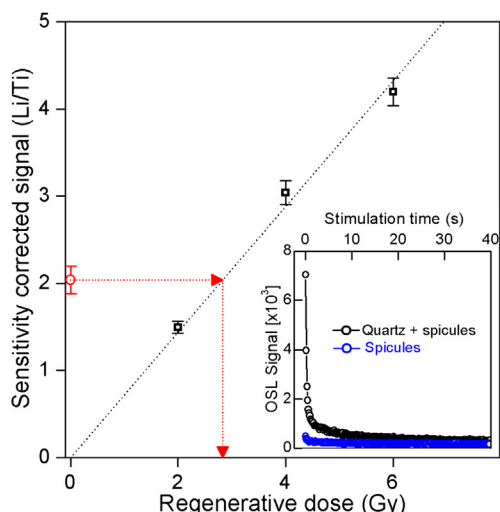


**Fig. 4.** Representative SAR growth curve for a single aliquot of quartz grains extracted from sample CSNH-68 for the determination of accumulated dose. The inset shows the OSL decay curves for a single aliquot of quartz grains mixed with spicules extracted from sample CSNH-68 and OSL decay curve for spicules extracted from freshwater sponge.

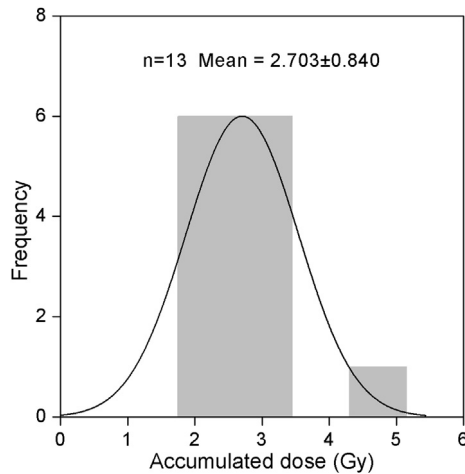


**Fig. 5.** The histograms of  $D_{ac}$  distribution of sample CSNH-68 for thirteen aliquots ( $n = 13$ ).

#### 3.4. EPR measurements

The EPR spectrum of the sample before chemical treatment with  $\text{HNO}_3$  is shown as an inset in Fig. 6. The main spectrum in Fig. 6 shows the observed spectrum after  $\text{HNO}_3$  chemical treatment. A narrow EPR line observed near  $g = 2.00035$  region was expanded, and this spectrum is also shown in Fig. 6. The inset spectrum intensity was higher, which shows that  $\text{HNO}_3$  is able to eliminate substantial concentrations of  $\text{Fe}^{3+}$  from the samples. In all the ceramic samples investigated, an intense and asymmetric line in the  $g = 2$  region was observed. This line is characteristic of  $\text{Fe}^{3+}$  in an octahedral site (Warashina et al., 1981; Bensimon et al., 1999; Presciutti et al., 2005; Mangueira et al., 2011). Furthermore, these ions are associated with hydrated species of  $\text{Fe}^{3+}$  which can be oxidized to  $\text{Fe}_x\text{O}_y$  or  $\text{FeOOH}$  (Bensimon et al., 2000). The EPR spectrum also shows another line in the region of  $g = 4.3$ , typical of  $\text{Fe}^{3+}$  in an orthorhombic site (Tani et al., 1997; Bensimon et al., 1999; Presciutti et al., 2005). The intensity of this line is about 40 times lower than the EPR line at  $g = 2.0$ . Another EPR line of low intensity was detected in the region 3458–3478 G. This line is

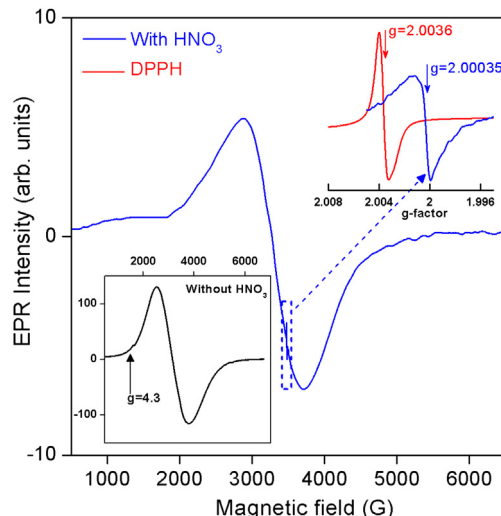


**Fig. 6.** EPR spectrum of sample CSNH-68 before (in the inset of figure) and after chemical treatments with  $\text{HNO}_3$ . DPPH gives  $g$ -value of the standard EPR signal.

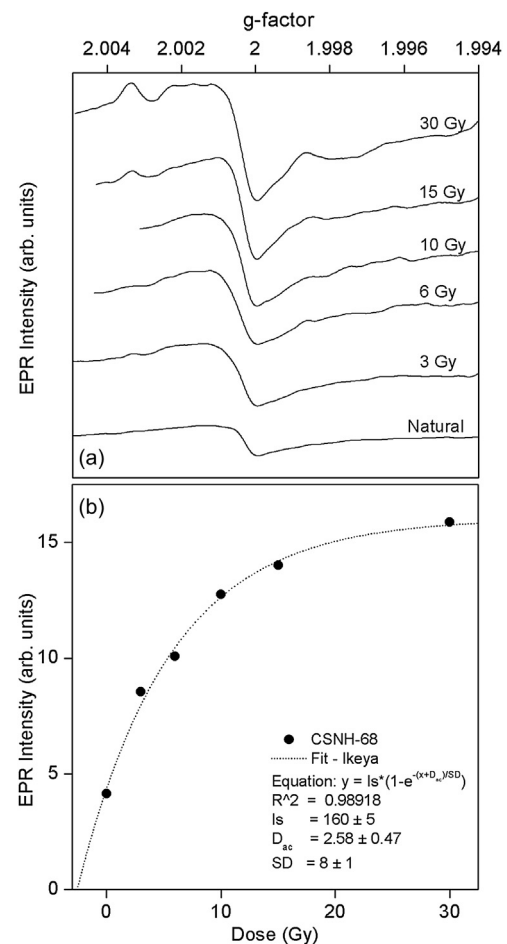


**Fig. 7.** (a) EPR spectrum of sample CSNH-68 after chemical treatments with  $\text{HNO}_3$  and irradiated with 3, 6, 10, 15 and 30 Gy. (b) Peak-to-peak EPR intensity versus gamma dose of sample CSNH-68.

shown in Fig. 6 with an expanded scale, and is characterized by a  $g$ -value of 2.00035. This signal is due to the well known E'-center in quartz and represents an electron bound to an oxygen vacancy (see Weeks, 1994; Bensimon et al., 2000). According to Chen et al. (1997), this species is thermally stable at temperatures below 500 °C regardless of heating time. The spicules obtained from freshwater sponges followed by irradiation with different gamma-doses did not exhibit any EPR signals in the region of 500–6500 G.

Iron contained in particles such as hematite can be washed out with  $\text{HNO}_3$  solution. Therefore, iron located in the structure of quartz grains cannot be eliminated. As shown in Fig. 6, the intensity of the EPR signal due to  $\text{Fe}^{3+}$  is much smaller, so that the signal at  $g = 2.00035$  due to E'-center can be observed. Fig. 7(a) shows EPR intensities of E'-centers with increasing dose in samples irradiated with radiation dose up to 30 Gy. Fig. 7(b) shows the behavior of the peak-to-peak intensity of the EPR signal at  $g = 2.00035$  as a function of the gamma dose. Applying the additive method, the accumulated dose  $D_{ac}$  was estimated to be about 2.57 Gy, comparable to the value obtained by OSL measurements.

Table 1 shows the accumulated dose, the annual dose rate and the age of ceramics using OSL and EPR techniques. The annual dose rate determination was carried out by measuring the concentrations of  $^{238}\text{U}$ ,  $^{232}\text{Th}$  and  $^{40}\text{K}$  in the ceramics using the neutron activation method. The results shown in Table 1 confirm the archaeological interpretation of the phases of occupation of the ancient people who lived in this region of the Amazon.

**Table 1**

Annual dose, accumulated dose, age (by EPR and OSL dating) and cultural phase of the ceramics.

Sample	$D_{an}$ (mGy/year)	EPR		OSL		Culture phase
		$D_{ac}$ (Gy)	Age (years)	$D_{ac}$ (Gy)	Age (years)	
CSNH-50	2.793	3.928 ± 0.240	604 ± 86	3.608 ± 0.840	718 ± 95	Manacapuru <sup>a</sup>
CSNH-67	2.261	2.648 ± 0.324	839 ± 86			Paredão <sup>b</sup>
CSNH-68	2.253	2.577 ± 0.468	866 ± 208	2.703 ± 0.840	810 ± 373	Paredão <sup>b</sup>
CSNH-69	2.242			1.061 ± 0.167	1537 ± 75	Paredão <sup>b</sup> Manacapuru <sup>a</sup> and Guarita <sup>c</sup>
CSNH-73	2.629			2.595 ± 0.442	1023 ± 168	Paredão <sup>b</sup>
CSNH-78	2.158	2.725 ± 0.455	745 ± 211	2.617 ± 0.590	797 ± 273	Paredão <sup>b</sup> Manacapuru <sup>a</sup> and Guarita <sup>c</sup>
CSNH-93	2.178			3.133 ± 0.477	571 ± 218	Paredão <sup>b</sup> Manacapuru <sup>a</sup> and Guarita <sup>c</sup>

<sup>a</sup> Manacapuru (500–900 years).<sup>b</sup> Paredão (700–1100 years).<sup>c</sup> Guarita (1000–1600 years).

## 4. Conclusions

Ceramics from Hatahara archaeological sites contain spicules as shown in Fig. 1(a). The spicules have large fluctuating TL intensity and interference in the TL-values of quartz grains and spicules obtained from ceramics, and hence TL dating was unsuitable. These spicules do not affect OSL and EPR measurements, and therefore these methods have been used in the present work. These techniques produced age values reasonably close to each other. Furthermore, these age-values are in conformity with the age-values of different archaeological phases found by Rebellato (2007).

## Acknowledgements

The authors wish to thank Ms. E. Somessari and Mr. C. Gaia, Instituto de Pesquisas Energeticas e Nucleares (IPEN/CNEN-SP), Brazil, for kindly carrying out the irradiation of the samples. This work was carried out with financial support from FAPESP and CNPq. NFC is sponsored by CNPq fellowships.

## References

Aitken, M.J., 1985. Thermoluminescence Dating. Academic Press, London.

Bartoll, J., Ikeya, M., 1997. Dating of pottery: a Trial. *Applied Radiation and Isotopes* 48, 981–984.

Bensimon, Y., Deroide, B., Clavel, S., Zanchetta, J.V., 1998. Electron spin resonance and dilatometric studies of ancient ceramics applied to the determination of firing temperature. *Japanese Journal of Applied Physics* 37, 4367–4372.

Bensimon, Y., Deroide, B., Dijoux, F., Martineau, M., 2000. Nature and thermal stability of paramagnetic defects in natural clay: a study by electron spin resonance. *Journal of Physics and Chemistry of Solids* 61, 1623–1632.

Bensimon, Y., Deroide, B., Zanchetta, J.V., 1999. Comparison between the electron paramagnetic resonance spectra obtained in X- and W-bands on a fired clay: a preliminary study. *Journal of Physics and Chemistry of Solids* 60, 813–818.

Botter-Jensen, L.B., Bulur, E., Duller, G.A.T., Murray, A.S., 2000. Advances in luminescence instrument systems. *Radiation Measurements* 32, 523–528.

Chen, Y., Feng, J., Gao, J., Grun, R., 1997. Investigation of the potential use of ESR signals in quartz for palaeothermometry. *Quaternary Science Reviews* 16, 495–499.

Costa, M.L., Kern, D.C., Pinto, A.H.E., Souza, J.R.T., 2004a. The ceramic artifacts in archaeological black earth (terra preta) from Lower Amazon region, Brazil: chemistry and geochemical evolution. *Acta Amazonica* 34, 375–386.

Costa, M.L., Kern, D.C., Pinto, A.H.E., Souza, J.R.T., 2004b. The ceramic artifacts in archaeological black earth (terra preta) from lower Amazon region, Brazil: mineralogy. *Acta Amazonica* 34, 165–178.

Duttine, M., Villeneuve, G., Poupeau, G., Rossi, A.M., Scorzelli, R.B., 2003. Electron spin resonance of  $Fe^{3+}$  ion in obsidians from Mediterranean islands. Application to provenance studies. *Journal of Non-crystalline Solids* 323, 193–199.

Ferretti, M., Forni, L., Oliva, C., Ponti, A., 2002. EPR study of iron-doped MFI zeolite and silicalite catalysts: effect of treatments after synthesis. *Research on Chemical Intermediates* 28, 101–116.

Ikeya, M., 1993. New Applications of Electron Spin Resonance. World Scientific, Singapore.

Machado, J.S., 2005. Montículos artificiais na Amazônia Central: um estudo de caso do Sítio Hatahara, Amazonas. Dissertation of Mestrado, University of São Paulo, São Paulo.

Mangueira, G.M., Toledo, R., Teixeira, S., Franco, R.W.A., 2011. A study of the firing temperature of archaeological pottery by X-ray diffraction and electron paramagnetic resonance. *Journal of Physics and Chemistry of Solids* 72, 90–96.

Murray, A.S., Wintle, A.G., 2000. Luminescence dating using an improved single aliquot regenerative-dose protocol. *Radiation Measurements* 32, 57–73.

Murray, A.S., Wintle, A.G., 2003. The single aliquot regenerative dose protocol: potential for improvements in reliability. *Radiation Measurements* 37, 377–381.

Nunes, K.P., 2009. Archaeometric Studies on the Hatahara Archaeological Site. Dissertation of Mestrado, Energy and Nuclear Research Institute, IPEN-CNEN/SP, University of São Paulo-USP, São Paulo.

Presciutti, F., Capitani, D., Sgamellotti, A., Brunetti, B.G., Costantino, F., Viel, S., Segre, A., 2005. Electron paramagnetic resonance, scanning electron microscopy with energy dispersion X-ray spectrometry, X-ray powder diffraction, and NMR characterization of iron-rich fired clays. *Journal of Physical Chemistry B* 109, 22147–22158.

Rebellato, L., 2007. Interpreting the Pottery Variability and the Chemical and Physical Signatures of the Soil in the Hatahara Archaeological Site, AM. Dissertation of mestrado, University of São Paulo, São Paulo.

Tani, A., Bartoll, J., Ikeya, M., Komura, K., Kajiwara, H., Fujimura, S., Kamada, T., Yokoyama, Y., 1997. ESR study of thermal history and dating of a stone tool. *Applications of Magnetic Resonance* 13, 561–569.

Warashina, T., Higashimura, T., Maeda, Y., 1981. Determination of the firing temperature of ancient pottery by means of ESR spectrometry. *British Museum Occasional Papers* 19, 117–123.

Watanabe, S., Farias, T.M.B., Gennari, R.F., Ferraz, G.M., Kunzli, R., Chubaci, J.F.D., 2008. Chemical process to separate iron oxides particles in pottery sample for EPR dating. *Spectrochimica Acta Part A* 71, 1261–1265.

Weeks, R.A., 1994. The many varieties of E' centers: a review. *Journal of Non-crystalline Solids* 179, 1–9.